Available online at www.sciencedirect.com
SCIENCE DIRECT®
PERGAMON
Organic Geochemistry 34 (2003) 483–497
Organic Geochemistry
www.elsevier.com/locate/orggeochem

Preservation of algaenan and proteinaceous material during the oxic decay of *Botryococcus braunii* as revealed by pyrolysis-gas chromatography/mass spectrometry and ^{13}C NMR spectroscopy

Reno T. Nguyen[a,1], H. Rodger Harvey[b], Xu Zang[a,2], Jasper D.H. van Heemst[a], Magdolna Hetényi[c], Patrick G. Hatcher[a,*]

[a]*Department of Chemistry, The Ohio State University, Columbus, OH 43210, USA*
[b]*Chesapeake Biological Laboratory, University of Maryland Center For Environmental Science, Solomons, MD 20688, USA*
[c]*University of Szeged, Department of Mineralogy, Geochemistry and Petrology, H-6701 Szeged, Hungary*

Received 9 March 2002; accepted 13 December 2002
(returned to author for revision 6 June 2002)

Abstract

Botryococcus braunii cells were grown until the late-stationary phase of growth and subsequently decomposed under oxic conditions for 201 days using a microbial consortium obtained from a freshwater lake. Degradation exhibited multi-G model kinetics, with a 'labile' fraction lost at a rate two to three times slower than those observed for the degradation of other previously studied phytoplankton, and a 'refractory' fraction lost even more slowly. Scanning electron microscopy of the 201-day detritus, as previously seen for the kerogen, indicates the preservation of cell wall material with loss of intracellular contents. Detrital samples analyzed by pyrolysis-gas chromatography/mass spectrometry (Py-GC/MS) and solid-state ramp-CPMAS ^{13}C NMR, however, indicates the preservation of highly aliphatic material, algaenan, as well as 'intrinsically labile' proteinaceous components. These results further support the encapsulation hypothesis that proteins may be sterically protected from enzymatic attack via intimate associations with refractory, macromolecular organic matter.

1. Introduction

Many crude oils are dominated by the presence of a large suite of alkanes with varying chain lengths, especially the high wax crude oils. It has been shown that these alkanes may originate from the cracking under suitable conditions of large aliphatic moieties (Tegelaar et al., 1989b) present in kerogens. Initially, these kerogens were thought to be derived from structures formed after random condensation and polymerization reactions of decomposing organic matter (Tissot and Welte, 1978). Subsequently, however, an alternative hypothesis on the formation of kerogen stated that refractory moieties present in different types of organic matter are selectively preserved and the more labile moieties are mineralized (Hatcher et al., 1983; Largeau et al., 1984, 1986; Goth et al., 1988; Tegelaar et al., 1989a). Many kerogens, including those of lacustrine Type I origin and

* Corresponding author. Tel.: +1-614-688-8799; fax: +1-614-688-5920.
E-mail address: hatcher@chemistry.ohio-state.edu (P.G. Hatcher).
[1] Present address: Grace Vydac, Hesperia, CA 92345, USA.
[2] Present address: Maxim Pharmaceuticals, 6650 Nancy Ridge Drive, San Diego, CA 92121, USA.

0146-6380/03/$ - see front matter © 2003 Elsevier Science Ltd. All rights reserved.
doi:10.1016/S0146-6380(02)00261-9

some of the more marine Type II origin, have a highly aliphatic character, similar to protective tissues present in some algal cell walls. Although these tissues usually comprise only a few percent of the total biomass of the algae, they are believed to be selectively preserved upon degradation and can therefore end up as major constituents in kerogen (Largeau et al., 1984, 1986; Goth et al., 1988; Derenne et al., 1991; Gillaizeau et al., 1996). These protective tissues are commonly referred to as algaenans (de Leeuw and Largeau, 1993). One freshwater to brackish water alga containing high amounts (up to 75% of its dry weight) of algaenans is *Botryococcus braunii*. It exists as three different races, *A*, *B* and *L*, with the race being determined based on the type of hydrocarbon synthesized (Berkaloff et al., 1983; Kadouri et al., 1988; Derenne et al., 1990; Metzger et al., 1989; Metzger and Casadevall, 1991). Cells of race *A* produce odd-carbon-numbered, dienic and trienic, normal hydrocarbons with carbon numbers $C_{25–33}$. Cells of race *B* produce triterpenic highly unsaturated C_nH_{2n-10} hydrocarbon with carbon numbers $C_{30–37}$, which are referred to as botryococcenes. Cells of race *L* produce exclusively one C_{40} isoprenoid hydrocarbon, which has been identified as lycopa-14(*E*),18(*E*)-diene. Algaenans originate from the polymerization of the high molecular mass lipids (Bertheas, 1999; Metzger and Largeau, 1999), and appear as a trilaminar sheath (Berkaloff et al., 1983) surrounding the classical, polysaccharidic cell wall (Gelin et al., 1999).

While there is clear evidence for the selective preservation hypothesis, it has only been recently that commonly considered labile, macromolecular constituents of algae have been found preserved along with refractory, macromolecular organic matter such as algaenans (Knicker and Hatcher, 1997; Nguyen and Harvey, 2001; Zang et. al., 2001). A 2D ^{13}C ^{15}N NMR study by Zang et al. (2001) of degraded *B. braunii* suggests that algaenans could play an important role in protecting peptide bonds from enzymatic attack. To further study the preservation of algal-derived algaenan and protein, decomposing *B. braunii* cells were studied by scanning electron microscopy, pyrolysis-gas chromatography/mass spectrometry and solid-state ramp-cross-polarization-magic-angle-spinning ^{13}C NMR.

2. Materials and methods

2.1. Algal cultures and degradation experiment

Details of algal growth and degradation are as previously described (Zang et al., 2001). Briefly, two cultures of *B. braunii* race A were grown in 20-L carboys with CHU medium (cultures obtained from Dr. C. Largeau and originally grown from the UTEX 572 strain that has been under study in the Largeau and Metzger groups; Metzger et al., 1989). One culture was grown in medium containing $NaH^{13}CO_3$ (98 at.%) which was added to obtain a ^{13}C isotopic enrichment of 20 at.%; the other was grown in medium containing $K^{15}NO_3$ for a ^{15}N enrichment of 99 at.% with no carbon isotopic enrichment. These isotopic labels were intended for our previous 2D ^{13}C ^{15}N NMR study, but here helped to discern algal-derived N-containing compounds in pyrolyzates.

The cultures were grown to late-stationary phase of growth, then mixed together in a 40-L carboy and allowed to degrade in a flow-through system with low dissolved organic carbon water from a natural, fresh water lake (Lake Lariat, Lusby, MD, USA). The mixing of the two cultures resulted in ca. 50 at.% and 5–10 at.% of the algae being ^{15}N- and ^{13}C-labeled, respectively. *B. braunii* was degraded for 201 days at a temperature of 25 °C in the dark, with sampling at predetermined time points. To minimize drawdown of the culture over the course of time, the sampling was not performed in replicate, but previous studies (Nguyen and Harvey, 1997) indicate an overall precision of about 5%. Bulk analyses included dry weight, particulate organic carbon (POC, precision of 1%) and particulate nitrogen (PN, precision of 2%). For bacterial counts, samples were fixed in glutaraldehyde (1% v/v final concentration made up in CHU medium, pH 7) and stored at 4 °C. Bacterial abundance was determined by flow cytometry (by P. del Giorgio at Horn Point Laboratory, University of Maryland). For pyrolysis GC/MS, samples were filtered onto pre-combusted glass-fiber filters (GF/F). For NMR work, cells and detritus were harvested by centrifugation (20,000×*g*, 30 min), rinsed in distilled water, frozen in liquid nitrogen, and then lyophilized.

2.2. Extraction of organic components from algal cells and detritus

For pyrolysis GC/MS and NMR, both whole and solvent-treated samples were analysed to characterize protein-derived material that could not be readily removed from the organic matrix. To remove lipids, pigments, and 'easily extractable' proteins, fresh algae and detritus were treated with various solvents as described by Zang et al. (2001). Briefly, lyophilized material was extracted with 10% (w/v) trichloroacetic acid in 90% acetone (containing 0.1% β-mercaptoethanol); acetone containing 0.1% β-mercaptoethanol (3 ×); 1:1 CH_2Cl_2: methanol (6 ×); and 0.1 N NaOH (1 h; 25 °C). The insoluble residue remaining after NaOH extraction was washed thoroughly with deionized water until the pH of the supernatant was neutral. A final extraction with 1:1 CH_2Cl_2: methanol was performed (2 ×) on the residue. The solvent-extracted residue was finally dried at 50 °C under a stream of nitrogen gas.

2.3. Pula kerogen

Kerogen was isolated by a sink-float method (Hetényi and Varsányi, 1976) which involves the use of a series of organic solvent mixtures of varying densities to separate relatively dense minerals from the less dense kerogen. Total organic carbon was determined after vapor phase acidification (Hedges and Stern, 1984). Untreated subsamples were used for total nitrogen determination.

2.4. Scanning electron microscopy (SEM)

Intact cells or degraded debris were centrifuged (2000×*g*; 20 min), rinsed in modified CHU medium, re-centrifuged, fixed in glutaraldehyde (1% v/v final concentration made up in CHU medium, pH 7) for 1 h at room temperature, and re-centrifuged. The cells and/or debris were rinsed briefly in CHU medium, re-centrifuged, flash frozen in liquid nitrogen, and lyophilized. Samples were stored at −70 °C prior to SEM. Algal samples and the kerogen were sputter coated with gold and observed under a Jeol 5200 SEM.

2.5. Pyrolysis-gas chromatography/mass spectrometry

Pyrolysis-gas chromatography/mass spectrometry (GC/MS) was performed using a Carlo Erba Mega 500 series GC operating in split mode (split 20:1), equipped with a Chemical Data Systems (CDS) pyrolysis interface and a 30-m DB 1701 column (0.25 mm i.d.; 0.25 μm film thickness). The interface temperature was held at 300 °C. Helium was used as a carrier gas, with a flow rate of 1 ml/min at a pressure of 100 kPa. The following oven temperature program was used: initial temperature of 40 °C (held for 2 min); and heating rate of 8 °C/min to a final temperature of 320 °C (held for 10 min). Samples were weighed (solvent-extracted residues) or cut out from the glass-fiber filters (untreated samples) and transferred to pre-combusted quartz tubes containing quartz spacers and silica wool. The tubes were then placed into the autosampler, which subsequently dropped them into a platinum resistance CDS-1000 coil pyroprobe. Samples were heated at a rate of 5 °C/ms to an indicated temperature of 615 °C when placed into the pyrolysis interface. This temperature was maintained for 15 s. The GC was connected to a Kratos MS-25 RFA mass spectrometer operated at 50 eV with a mass range of m/z 30–550 and a cycle time of 0.33 s (150 μA emission current; 150 °C ionization source temperature). Data acquisition and analysis were performed using a Dart/Kratos Mach 3 data system. Pyrolysis products were identified based on their mass spectra and GC retention times, by comparison with the NIST mass spectral library and published GC/MS data (e.g., Stankiewicz et al., 1997).

2.6. Solid-state ^{13}C NMR

Samples were subjected to solid-state ^{13}C NMR spectroscopy, using cross-polarization-magic-angle spinning (CPMAS), a ramp-CP procedure, and two-pulse phase modulation (TPPM). The ramp-CPMAS pulse program was employed as described by Cook and Langford (1998), but with the carbon spin-locked conditions ramped rather than that of the proton channel. According to Cook and Langford (1998), either channel can be ramped.

Samples were weighed and placed in 4-mm diameter rotors with Kel-F® caps. The rotors were generally packed with 100 mg dry weight per sample. They were spun at 13 kHz at the magic angle (54.7°) in the probe of a Bruker DMX-300 MHz NMR operating at 75.48 MHz for carbon. A cross-polarization pulse sequence with 2 ms contact time and 1 s recycle delay time was used and approximately 10^5 acquisitions (scans) were accumulated to obtain the spectra. Exactly 2048 data points were acquired and zero-filled to 8192 total data points prior to filtering with 100 Hz line broadening and Fourier transformation. The chemical shifts were plotted using the carboxyl signal of glycine as external standard (176.03 ppm).

3. Results and discussion

3.1. Kinetics of degradation

Algal material at the start of the degradation experiment had a dry biomass, POC, and PN content of 650, 283, and 35.5 mg l^{-1}, respectively (Fig. 1A). The culture vessel also contained a high concentration of dissolved organic carbon (35 mg l^{-1}), which could be attributed largely to the production of polysaccharides by the algae during growth. The amount of extracellular polysaccharides released in the culture medium by different strains of *B. braunii* has been observed to range from 250 mg l^{-1} to 1 g l^{-1} (Allard and Casadevall, 1990). Loss of particulate organic matter over the first 30 days was rapid, slowing over the next 171 days of the incubation. First-order decay constants of 6.6 $year^{-1}$ for PN to 8.5 $year^{-1}$ for dry weight were observed for the 'labile' fraction, while rate constants of 1.8–3.2 $year^{-1}$ characterized the 'refractory' fraction (Table 1). For the first 30 days of *B. braunii* decay, the atomic C:N of organic matter showed little variation at 9.0±0.07 (mean±S.E.; Fig. 1B), but increased steadily to an atomic C:N of 16.7 by 201 days. By the end of the 201-day incubation, 14% of PN and 26% of the initial POC remained (Table 1). On a weight per weight basis the residual organic matter contained 55.3% OC and 3.86% N. By comparison, the Pula kerogen, which underwent diagenetic maturation during burial, was

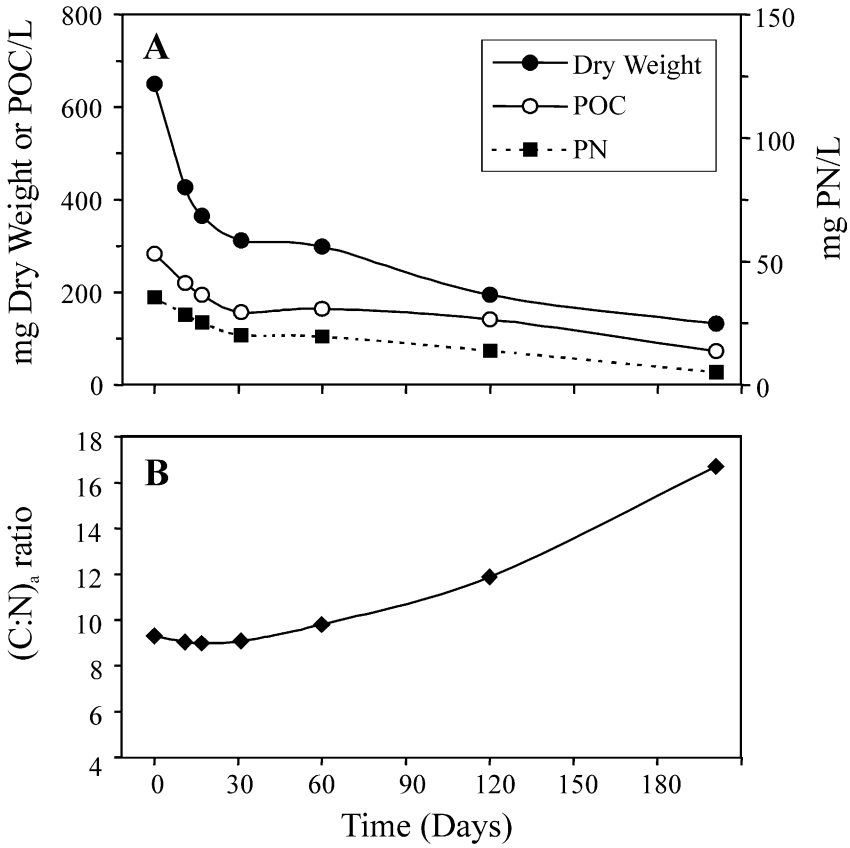

Fig. 1. Time course of (A) dry weight, particulate organic carbon, and particulate nitrogen; and (B) the atomic carbon-to-nitrogen ratio during the oxic decay of *B. braunii*. Samples were not collected in duplicate but elemental analyses were performed in triplicate. Errors are less than or equal to the data point size shown.

Table 1
Experimentally determined first-order decay constants [k, year^{-1} ($\pm$95% CL)], determination coefficients (r^2), and percentage of initial material degraded (% deg) for particulate organic carbon, particulate nitrogen, and dry weight during the oxic decay of *B. braunii*

Fraction	'Labile' fraction[a]			'Refractory' fraction		
	k_1	r^2	Deg. (%)	k_2	r^2	Deg. (%)
Particulate organic carbon	6.9 (2.4)	0.99	45	1.8 (1.0)	0.86	74
Particulate nitrogen	6.6 (1.3)	1.0	43	3.2 (1.2)	0.93	86
Dry weight	8.5 (8.3)	0.91	52	1.9 (0.6)	0.96	80

[a] The labile fraction represents material lost up until day 30 of the 201-day incubation where a sharp break was observed in loss rates (see Fig. 1).

more carbon-rich, but nitrogen-poor, with an OC and a N content of 65.8 and 0.66%, respectively, for an $(C:N)_a$ of 116.

The 'labile' fraction of *B. braunii* was lost 1.9–3.5 times slower than observed for previously studied phytoplankton (Fig. 2; and Nguyen and Harvey, 1997). The marine phytoplankton species previously studied were from three different classes: Bacillarophyceae (diatoms), Dinophyceae (dinoflagellates), and Cyanophyceae (cyanobacteria). Decay constants for the 'labile' and 'refractory' fraction of *B. braunii* are shown as k_1 and k_2, respectively. For the first three phytoplankton, constants for the decay were calculated over the entire incubation period (Nguyen and Harvey, 1997). For *T.*

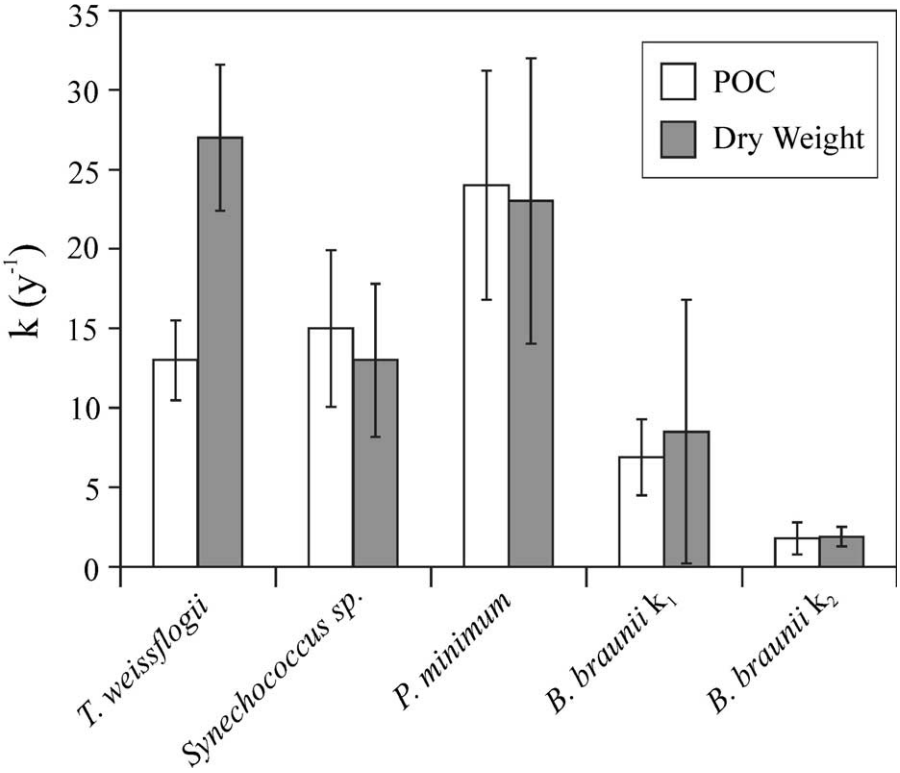

Fig. 2. Comparison of first-order decay constants (±95% CL calculated by a least squares regression analysis) for particulate organic carbon and dry weight during the oxic degradation of four phytoplankton species: *Thalassiosira weissflogii* (diatom), *Synechococcus* sp. (cyanobacterium), *Prorocentrum minimum* (dinoflagellate), and *B. braunii* (green alga).

weissflogii decay, the large difference between k values for POC and dry weight is likely due to silica dissolution. Bacterial cell numbers typically increased from 10^5 or 10^6 to 10^7 cells ml^{-1} just prior to or during the most rapid time of decay of the diatom, cyanobacterium and dinoflagellate cells (Harvey and Macko, 1997). Bacterial numbers remained relatively constant during the 201-day decay of *B. braunii*, averaging $(6.4\pm1.1)\times10^6$ cells ml^{-1}.

B. braunii and these marine phytoplankton possess distinctly different cell wall matrices. Diatoms possess silica-based cell walls that also include biomacromolecules such as glycoproteins (Kröger et al., 1994) and chitin (polymer of *N*-acetylglucosamine; Smucker and Dawson, 1986). Dinoflagellates have cell walls composed principally of cellulose (Brock and Madigan, 1984). The cell wall of some cyanobacteria is similar to that of Gram-negative bacteria, which have peptidoglycan and lipopolysaccharide in their walls (Brock and Madigan, 1984). While small differences in culture or experimental decay conditions (temperature, bacterial communities, marine vs freshwater, etc.) could explain some of the differences in degradation rates amongst the phytoplankton species, the non-hydrolyzable and insoluble nature of the algaenan matrix of *B. braunii* likely appears responsible for the slower rate of organic matter degradation of this alga.

3.2. Morphological changes during diagenesis

SEM analysis of late-stationary phase *B. braunii* (day 0) indicates a typical cell size of ~10 μm (Fig. 3A) which was confirmed by light microscopy. Colonies (aggregates of cells) were not observed, likely a consequence of the vigorous aeration used during growth. Occasional 'ghost' cells were observed (Fig. 3B), as some algae had reached senescence and lost their intracellular contents. Analysis of algal cells after 201 days of degradation indicates the preservation of cell wall material, but little of the original cell morphology (Fig. 3C). As previously observed by Derenne et al. (1997), the 4-Ma Pula kerogen exhibited distinct, fossilized colonies with preserved cell wall material and morphology despite the loss of intracellular contents (Fig. 3D). Although cell wall material was retained in both, different depositional or degradation conditions most likely have led to the dissimilar appearance of *B. braunii* cell walls in the 201-day-old detritus versus the 4-Ma kerogen.

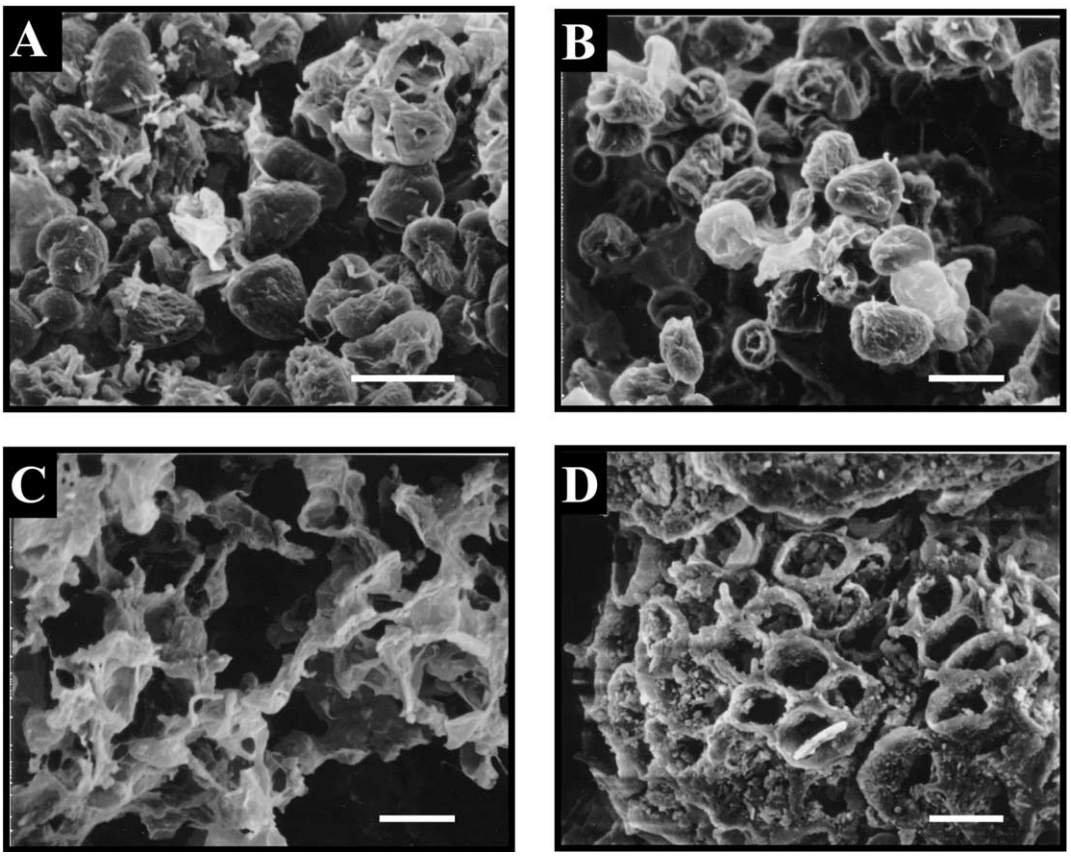

Fig. 3. Scanning electron micrographs of *B. braunii* during different stages of degradation. (A, B) Two views of stationary-phase intact and ghost cells; (C) 201-day-degraded cells; (D) 4-Ma Pula kerogen comprised of fossilized colony of cells with the algaenan cell wall component preserved. White bar indicates 10 μm.

3.3. Pyrolysis GC/MS

3.3.1. Stationary-phase algae

Numerous aliphatic compounds were identified in the pyrolysis total ion chromatogram of stationary-phase *B. braunii* cells (day 0; Fig. 4A; Table 2). A phytadiene (39) and $C_{16:0}$ and $C_{18:1}$ fatty acids (43, 45) are the predominant peaks. Prist-1-ene (36), phytenes (37, 38) and phytadienes (39, 40, 41) with varying unsaturation sites, and phytol (44) are the primary chlorophyll-derived pyrolysis products in fresh algal material. The tetrapyrrole structure of chlorophyll is too stable to be pyrolyzed at 615 °C; however, the esterified phytol is easily cleaved by pyrolysis, and it is then transformed to a phytadiene via an elimination mechanism. The $C_{16:0}$ and $C_{18:1}$ fatty acids in the pyrolyzate of *B. braunii* cells previously have been observed to be the dominant fatty acids in stationary-phase green algae (Thompson, 1996). In addition to the typical fatty acids, the fatty amides hexadecanamide (48) and 9-octadecenamide (49) are present in *B. braunii*. These compounds have been found in freshwater green algae (Dembitsky et al., 2000) and seagrass (Kawasaki et al., 1998). Due to the algaenan cell wall, alkanes/alkene doublets from C_6 to C_{31} are contributors to the total ion chromatogram of the algae and become more dominant with increasing time of degradation. Alkadienes (e.g., $C_{25:2}$, $C_{29:2}$, and $C_{31:2}$) characteristic of *B. braunii* race *A* (Derenne et al., 1990) were identified as well.

Protein-derived pyrolysis products including toluene (5), phenol (25), indole (34) and 5-methylindole (35) are abundant relative to the *n*-alkane/alk-1-ene products in the late stationary-phase algae (Fig. 4A). Minor protein-derived products included pyridine (6), a pyridine derivative (7), 1-methylpyrrole (13), benzeneacetonitrile (28), succinimide (31), and benzenepropanenitrile (32). However, their relative contributions are more significant in the post-solvent extraction residues of the stationary-phase algae (data not shown). This indicates that the NaOH extraction step could not remove all of the proteins, and that the protein-derived pyrolysis products are enriched after the extensive removal of lipids

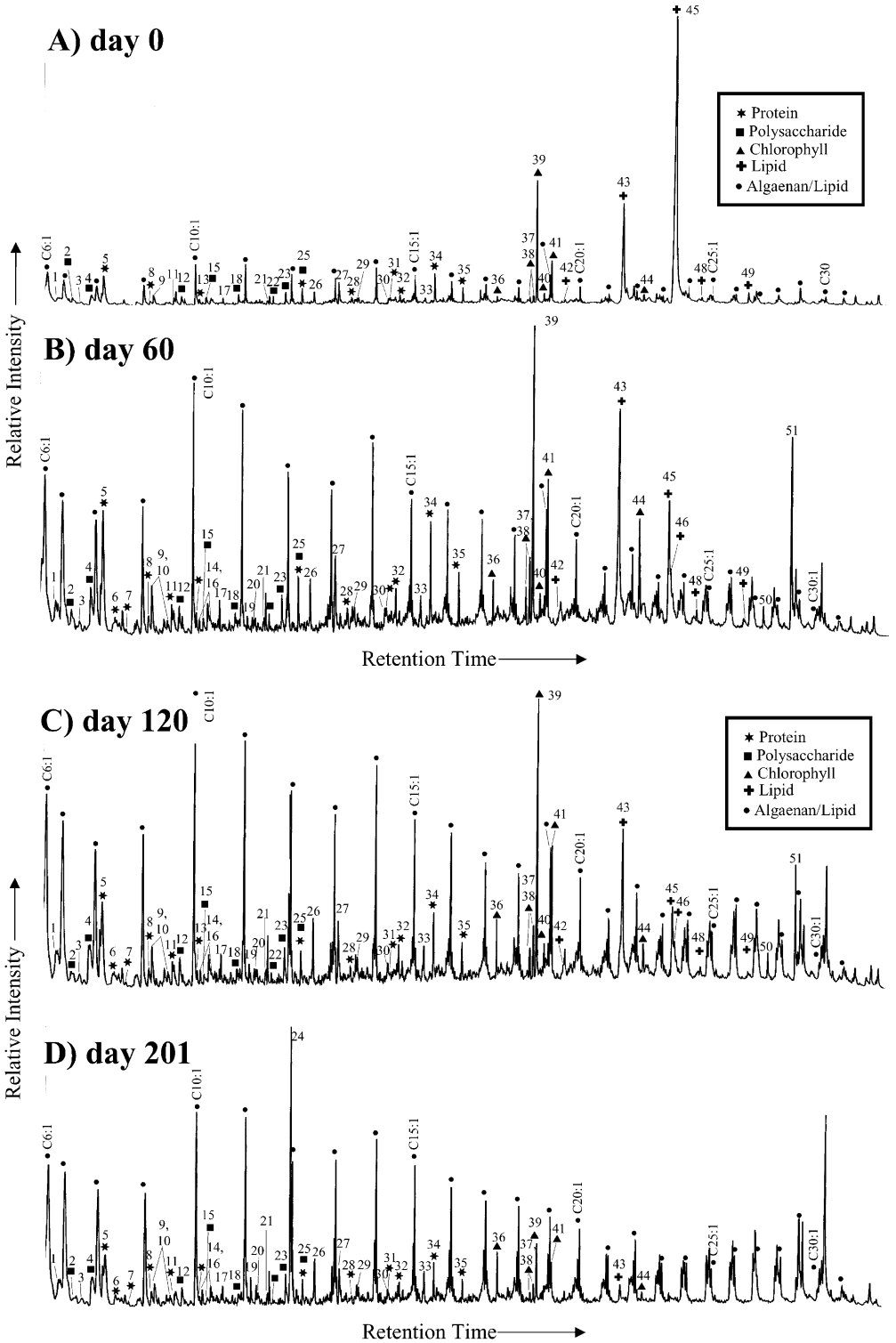

Fig. 4. Total reconstructed ion chromatograms of pyrolyzates (615 °C for 15 s) of (A) stationary-phase *B. braunii* cells, day 0, and of the decomposing suspension at (B) day 60, (C) day 120, (D) day 201. Refer to Table 2 for peak assignments. Possible origins of various peaks are indicated by symbols. Filled circles indicate the *n*-alkane/*n*-alk-1-ene peaks. These doublets are not completely resolved due to the polarity of the column.

Table 2
Non- *n*-alkane/alk-1-ene pyrolysis products of *B. braunii* decay samples. Numbers underlined indicate the molecular mass and in bold indicate base peak. Peak numbers correspond to those peaks labeled for chromatograms in Fig. 4

Peak No.	Compound	Potential origin	Characteristic fragment ions (m/z)[b]	($M^+ + 1$) from ^{15}N Labeling
1	4-Methylcyclopentene	–	82, 81, **67**, 54, 53, 41, 39	
2	3-Methylbutanal	Polysaccharide	86, 71, 58, 57, **44**, 43, 41	
3	4-Methylcyclohexene	–	96, **81**, 68, 67, 55, 54	
4	Acetic acid	Polysaccharide	60, 45, **43**	
5	Methylbenzene (toluene)	Phenylalanine	92, **91**, 65, 51	
6	Pyridine	Alanine, aminosugar	**79**, 52, 51, 50	m/z 80
7	Pyridine derivative	Alanine, aminosugar		
8	Ethylbenzene	Phenylalanine	106, **91**, 77, 65, 51	
9	1,4- and 1,3-Dimethylbenzene	Lignin?	106, 105, **91**, 77, 65, 51	
10	1,2-Dimethylbenzene	Lignin?	106, 105, **91**, 77, 65, 51	
11	Styrene	Phenylalanine	**104**, 103, 78, 51	
12	2-Cyclopentenone	Polysaccharide	**82**, 54, 53, **39**	
13	1-Methylpyrrole	Proline, hydroxyproline	**81**, 80, 53, 42	m/z 82
14	C3-Alkylbenzene	-	120, **105**, 91, 79, 78, 77	
15	2-(Hydroxymethyl)furan	Polysaccharide	**98**, 97, 81, 70, 69, 39	
16	C3-Alkylbenzene	–	120, **105**, 91, 79, 78, 77	
17	Limonene	–	136, 121, 107, 93, 79, **68**, 53	
18	2,3-Dihydro-5-methylfuran-2-one	Polysaccharide	98, 70, **55**, 43	
19	1-Pentyl-2-propylcyclopropane	–	154, 126, 111, 97, 84, 69, **55**	
20	Indene	–	**116**, 115, 89, 75, 63, 51	
21	Transdecahydronaphthalene	–	138, 123, 109, 96, 82, 68, 55, **41**	
22	3-Methyl-5-methylidene-2(5H) furanone	Polysaccharide	**110**, 82, 68, 54, 42	
23	2-Hydroxy-3-methyl-2-cyclopenten-1-one	Polysaccharide	**112**, 84, 83, 69, 55	
24	*n*-Nonaldehyde and 12:0 alkane	Lipid?, algaenan	142, 124, 114, 98, 82, 70, **57**, 43, 41 (nonaldehyde)	
25	Phenol	Tyrosine, polysaccharide	**94**, 66, 65	
26	Cyclododecene	–	166, 138, 123, 109, 96, 82, **67**, 55	
27	3-Methylphenol	Lignin?	**108**, 107, 79, 77	
28	Benzeneacetonitrile	Phenylalanine	**117**, 116, 90, 89	m/z 118
29	3,5-Dimethylphenol	Lignin?	**122**, 121, 107, 91, 79, 78, 77	
30	1,2-Dihydro-1,1,6-trimethylnaphthalene	–	172, **157**, 142, 128, 115, 106, 91	
31	2,5-Pyrrolidinedione (succinimide)	Asparagine	**99**, 70, 56, 42	m/z 100
32	Benzenepropanenitrile	Phenylalanine	131, **91**, 77, 65, 51	m/z 132
33	2,6-Dimethoxyphenol	Lignin?	**154**, 139, 111, 93, 65	
34	Indole	Tryptophan	**117**, 90, 89, 63	m/z 118
35	5-Methylindole	Tryptophan	**131**, 130, 103, 77	m/z 132
36	Prist-1-ene[a]	Chlorophyll	266, 196, 140, 126, 111, 98, 83, 69, 56, 43	
37	Phytene′[a]	Chlorophyll	280, 210, 196, 140, 126, 125, 111, 97, 83, 70, 69, 57, 55, **43**	
38	Phytene″[a]	Chlorophyll	280, 210, 196, 140, 126, 125, 111, 97, 85, **70**, 69, 57, 55, 43	
39	Phytadiene′[a]	Chlorophyll	278, 263, 208, 179, 123, 109, 95, 82, **68**, 57	
40	Phytadiene″[a]	Chlorophyll	278, 266, 208, 179, 123, 109, 95, **82**, 68, 57	
41	Phytadiene‴[a]	Chlorophyll	278, 264, 208, 179, 123, 109, 95, **82**, 68, 57	
42	14:0 Fatty acid	Lipid	228, 199, 185, 171, 143, 129, **73**, 60	
43	16:0 Fatty acid	Lipid	**256**, 213, 185, 129, 73, 60	
44	Phytol	Chlorophyll	296, 278, 196, 123, 111, 95, 81, **71**, 57, 43	
45	18:1 Fatty acid	Lipid	282, 264, 222, 180, 125, 111, 97, 83, 69, **55**	
46	18:0 Fatty acid	Lipid	284, 241, 185, 129, 97, 83, 73, 60, **43**	
47	18:2 Fatty acid	Lipid	280, 264, 196, 182, 150, 137, 124, 110, 95, 81, **67**, 55	
48	Hexadecanamide	Lipid	255, 226, 212, 128, 114, 86, 72, **59**	m/z 256
49	(*Z*)-9-Octadecenamide	Lipid	281, 154, 126, 97, 72, **59**, 55, 43	m/z 282
50	bis(2-Ethylhexyl)phthalate	Contaminant	390, 279, 167, **149**, 113, 71, 57	
51	Squalene	Contaminant	410, 367, 341, 299, 273, 231, 191, 149, 137, 121, 95, **81**, 69	

[a] Phytenes and phytadienes with different unsaturation sites were detected. Prist-1-ene has not been previously identified from chlorophyll, but chlorophyll is the only likely source in this study.
[b] Fragment ions for unlabeled compounds.

Table 3
Relative distribution of pyrolysis products from compound classes during *B. braunii* decay

	Relative distribution (%)					
	0 days	11 days	30 days	60 days	120 days	201 days
Protein derived						
Toluene	30.2	46.4	39.4	35.9	32.5	40.0
Pyridine	2.8	3.5	4.2	3.7	3.8	7.7
Pyridine derivative	0.9	2.0	0.3	2.2	2.9	3.3
Ethylbenzene	4.9	4.0	6.7	5.5	6.8	8.3
Styrene	4.9	2.9	2.9	4.0	4.8	3.2
1-Methylpyrrole	4.8	3.0	2.2	3.8	4.2	3.8
Phenol	8.3	5.7	6.4	7.0	7.8	7.2
Benzeneacetonitrile	6.7	3.1	3.9	5.0	6.9	3.6
Succinimide	4.5	2.9	4.0	5.7	3.7	3.6
Benzenepropanenitrile	5.8	4.2	6.6	5.5	7.1	5.3
Indole	16.7	14.9	16.7	14.7	14.5	9.0
5-Methylindole	9.4	7.3	6.8	7.0	8.5	5.1
Polysaccharide derived						
3-Methylbutanal	18.6	17.9	17.6	13.9	13.7	15.2
Acetic acid	23.1	38.4	41.4	40.2	31.6	42.1
2-Cyclopentenone	12.3	11.0	12.7	13.1	16.3	13.5
2-(Hydroxymethyl)furan	10.3	4.9	4.8	7.6	8.7	9.1
2,3-Dihydro-5-methylfuran-2-one	12.6	10.1	6.7	7.3	6.3	7.3
3-Methyl-5-methyliden-2(5H)-furanone	7.0	3.7	2.8	4.5	5.3	2.3
2-Hydroxy-3-methyl-2-cyclopenten-1-one	13.7	14.0	14.0	13.4	18.1	10.5
Chlorophyll derived						
Prist-1-ene	5.3	4.0	4.2	6.4	10.7	20.5
Phytene′	5.6	3.2	3.6	5.5	7.0	5.9
Phytene″	7.7	5.8	6.3	8.8	10.3	8.3
Phytadiene′	43.0	52.5	41.3	37.2	37.7	28.0
Phytadiene″	9.7	4.7	6.9	5.5	7.7	8.3
Phytadiene‴	17.9	18.7	20.5	17.1	17.4	22.8
Phytol	10.8	11.1	17.3	19.5	9.2	6.2
Lipid derived						
14:0 Fatty acid	1.6	0.4	0.2	3.1	5.8	0
16:0 Fatty acid	19.8	42.1	58.6	62.4	58.1	100
18:1 Fatty acid	72.4	53.0	36.0	30.3	24.3	0
Hexadecanamide	2.8	1.7	3.2	3.0	8.1	0
(*Z*)-9-Octadecenamide	3.4	2.9	2.0	1.2	3.7	0
Algaenan/lipid derived alkenes						
6:1	20.8	15.3	21.6	17.9	16.5	18.1
7:1	9.9	13.0	11.9	11.4	11.4	13.4
8:1	7.1	9.9	8.3	9.0	7.8	9.4
9:1	4.5	5.8	5.8	6.0	5.5	6.5
10:1	6.0	6.8	6.7	7.3	5.9	6.9
11:1	3.8	4.7	4.6	4.8	4.3	4.4
12:1	2.9	3.3	3.1	3.4	3.2	3.5
13:1	2.8	3.0	2.9	3.3	3.1	3.2
14:1	3.7	3.7	3.8	4.3	3.8	3.5
15:1	3.2	3.1	2.9	3.3	3.2	3.1
16:1	2.9	2.5	2.7	2.9	2.6	2.7
17:1	2.6	2.6	2.6	2.9	2.6	2.6
18:1	2.3	2.2	2.1	2.4	2.4	2.3

(*continued on next page*)

Table 3 (*continued*)

	Relative distribution (%)					
	0 days	11 days	30 days	60 days	120 days	201 days
19:1	3.6	3.7	2.7	3.1	2.9	2.1
20:1	2.8	2.2	2.2	2.5	2.6	1.8
21:1	1.7	1.2	1.2	1.6	1.7	1.3
22:1	2.6	1.9	2.0	2.4	2.3	1.7
23:1	1.8	1.1	1.1	1.4	1.6	1.0
24:1	3.2	1.9	1.6	1.8	2.3	1.3
25:1	3.1	1.4	1.4	1.5	2.2	1.2
26:1	3.8	1.4	1.4	1.8	3.0	1.6
27:1	1.9	0.9	1.1	0.9	3.4	0.9
28:1	2.4	2.3	1.2	1.1	1.8	2.0
29:1	3.2	3.6	3.4	1.7	1.2	3.6
30:1	2.7	1.1	0.6	0.8	1.3	0.8
31:1	3.5	1.5	1.1	0.5	1.3	1.1

by the organic solvents. Incomplete removal of proteins suggests that an important fraction of proteins are retained within the refractory cell wall algaenans.

An examination of the mass spectra indicates that all N-containing pyrolysis products are enriched in ^{15}N (Table 2) as expected, based on the fact that we grew half of the algal population on 99 at.% $K^{15}NO_3$. Compound identification was based on both best matches with the NIST mass spectral library and retention times of corresponding unlabeled compounds. The ^{15}N-enriched compounds include the protein-derived products (Table 2) as well as the fatty amides. In all cases, both the M^+ and ($M^+ + 1$) ions are observed.

Polysaccharide-derived pyrolysis products such as 3-methylbutanal (2), acetic acid (4), 2-cyclopentanone (12), 2-(hydroxymethyl) furan (15), 2,3-dihydro-5-methylfuran-2-one (18), 3-methyl-5-methylidene-2(5H) furanone (22), and 2-hydroxy-3-methyl-2-cyclopenten-1-one (23) are generally in low abundance in stationary-phase algae (Fig. 4A). As observed for the protein markers, the relative contributions of the polysaccharide markers are more significant in the post-solvent residues of the stationary-phase algae (data not shown), due to their enrichment after the extensive removal of lipids by the organic solvents.

Some compounds not previously described in pyrolysis GC traces of *B. braunii* were identified. For example, limonene (17), a monocyclic monoterpene known to be synthesized by various higher plants was detected in the green algae. This terpene may represent either a natural biosynthetic component or an artefact of the pyrolysis. In addition, although commonly ascribed as lignin-derived compounds, the pyrolysis products dimethybenzenes (9,10), 3-methylphenol (27), 3,5-dimethylphenol (29), and 2,6-dimethoxyphenol (33) were identified in the algae. It is unlikely that lignin was present in our samples, since the freshwater source for the degradation experiment was centrifuged and filtered to exclude vascular plant debris. We also filtered samples to collect material for pyrolysis during the degradation period; thus, dissolved contributions of lignin should have been minor. Although these compounds may not be unequivocal markers for lignin, their origin in the case of the *B. braunii* samples is unknown.

3.3.2. Changes during oxic decay

Significant changes in organic matter composition were observed for lipid and chlorophyll-derived compounds (Fig. 4A–D and Table 3). The $C_{16:0}$ and $C_{18:1}$ fatty acids comprised 20 and 72% of all fatty acids/amides at day 0, respectively (Table 3). During the oxic decay of *B. braunii* cells, the $C_{16:0}$ and $C_{18:1}$ fatty acids decreased rapidly among the fatty acids, with only the $C_{16:0}$ fatty acid detectable in the 201-day detritus (Fig. 4D). Bacterial-C comprised ~1% of total particulate organic carbon during the incubation period and may account for the lack of a strong bacterial fatty acid signal. The fatty amides were observed until at least day 120, but they were not detectable in the 201-day old detritus. Over a period of 201 days, prist-1-ene generally increased from 5 to 20% of those compounds believed to be derived from chlorophyll. We include prist-1-ene in this group, even though it has not specifically been identified to be derived from chlorophyll, because we envision no possible source other than the algae. The distribution of phytenes did not change much, while the major phytadiene (39) decreased from 43 to 28% of chlorophyll-derived compounds; and phytol increased from 11 to 20% for the first 60 days, and then decreased to 6% by 201 days (Table 3). Nonaldehyde (24) was only detected in the 201-day old detritus, although it coeluted with dodecane ($C_{12:0}$). Long-chain aldehydes have been shown to be formed enzymatically from fatty acids in various photosynthetic organisms (Kawasaki et

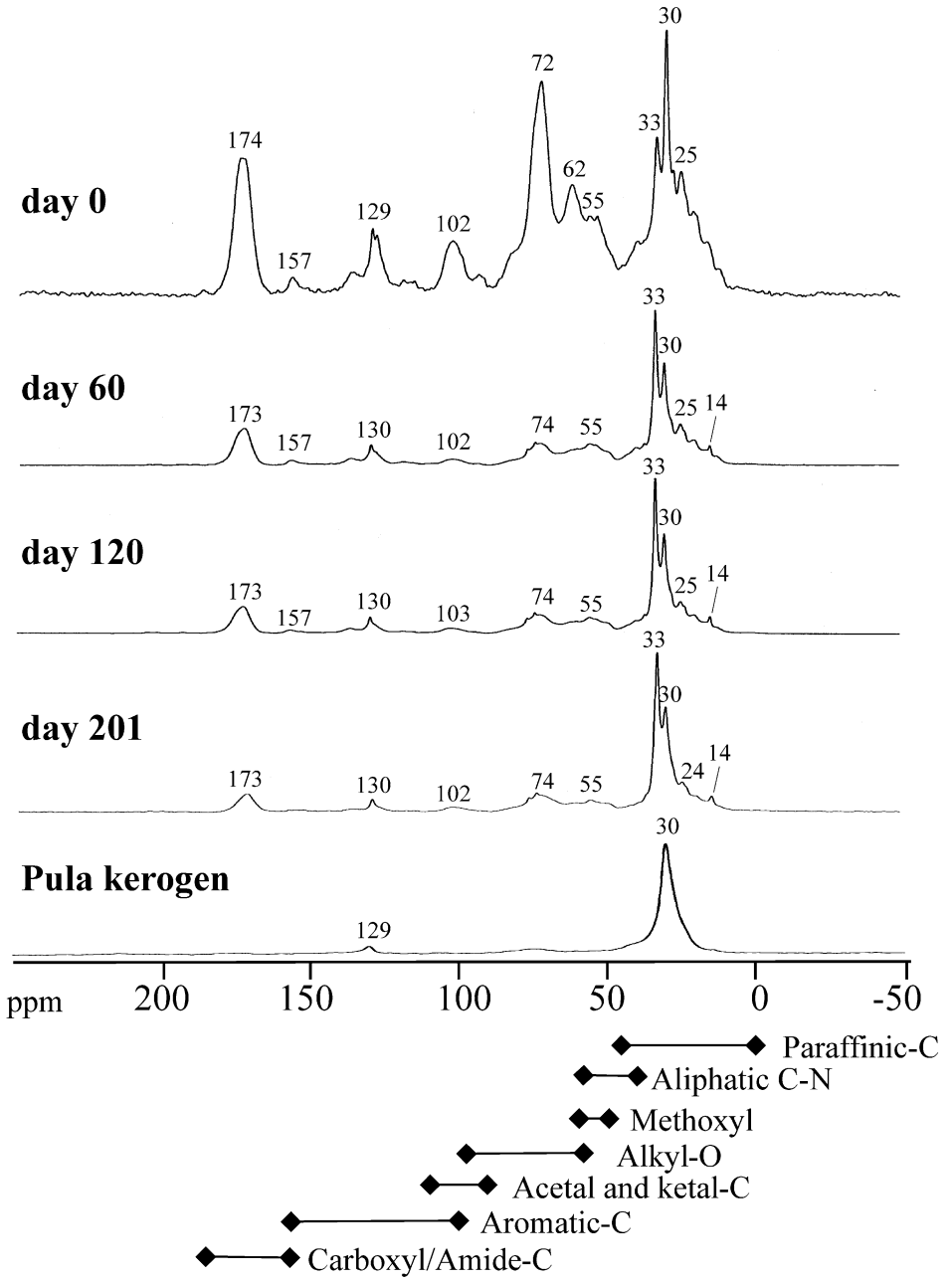

Fig. 5. Solid-state ^{13}C CPMAS NMR spectra of whole samples of stationary-phase *B. braunii* (day 0), the decomposing suspension, and Pula kerogen.

al., 1998), but the origin of this compound remains unclear. Other lipid components detected in the pyrolysis GC traces included squalene (51), a triterpene. This compound is likely a contaminant in the day 60 and 120 samples, as it is found in human surface lipids and was present along with a phthalate (50).

During the degradation sequence, there is a selective enrichment of a highly aliphatic macromolecular material in the residual organic matter as is revealed by the increasing intensity of the *n*-alkane/alk-1-ene doublets (Fig. 4). Although initially present in lower relative amounts in the pyrolyzate of the stationary-phase algal cells (Fig. 4A, day 0), the intensity of the *n*-alkane/alk-1-ene doublets dominates the entire chromatogram of the pyrolyzate of the filtered suspension after 201 days of decomposition (Fig. 4D). This indicates that the organic

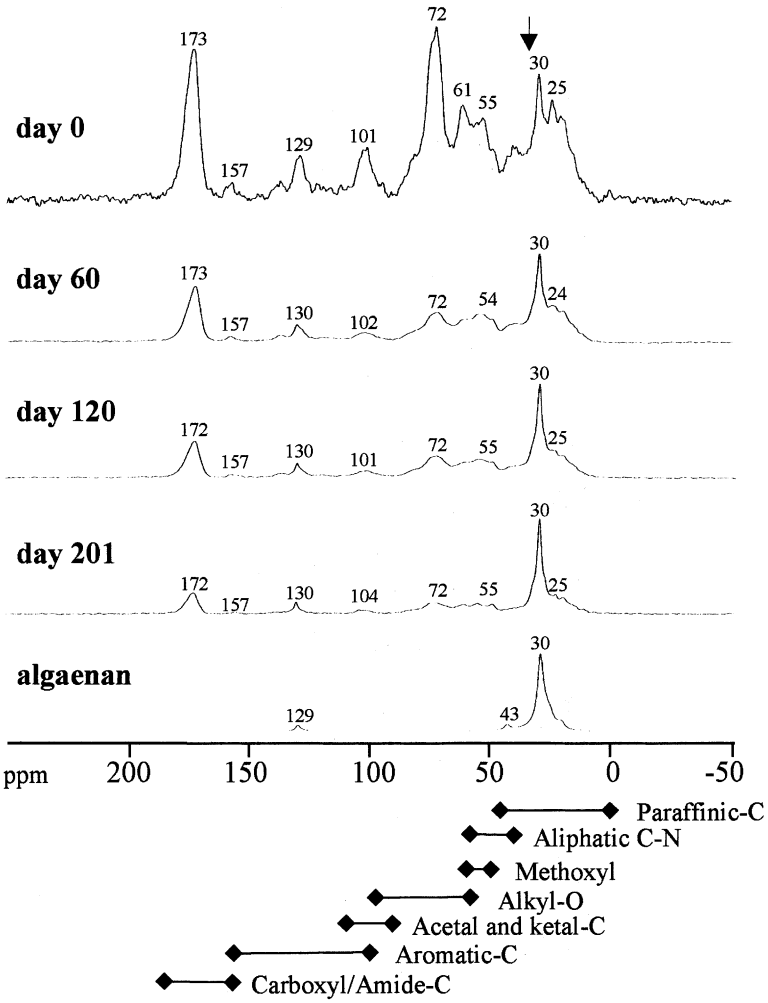

Fig. 6. Solid-state ^{13}C CPMAS NMR spectra of stationary-phase (day 0) and decomposing *B. braunii* residues after sequential solvent extractions. Algaenan was isolated from stationary-phase algae by a sodium paraperiodate procedure (Zelibor et al., 1988). Arrow emphasizes the lack of a 33-ppm peak seen in spectra of whole samples (Fig. 5).

matter of the filtered suspension after 201 days of decomposition is comprised mainly of algaenan, consistent with the NMR data discussed below. The relative enrichment of algaenan in the organic matter of the decomposing algae, as shown in the total ion chromatograms (Fig. 4D), occurs during the observed decrease in total dry weight and particulate organic carbon (Fig. 1A). These results indicate the more rapid decomposition of materials such as proteins and carbohydrates compared to materials like algaenan. After 201 days of oxic decay, 80% of the initial algal biomass had been decomposed. The enrichment in algaenan is also seen by an increase in the atomic carbon-to-nitrogen ratio of particles during the decay, from 9.1 for late-stationary phase cells to 16.7 for the 201-day old detritus (Fig. 1B).

Protein-derived pyrolysis products were abundant relative to the *n*-alkane/alk-1-ene products in the detritus from the early stages of diagenesis. After 60 days, the contributions of proteinaceous material to the pyrolyzates decreased significantly. Amongst the protein-derived compounds, the relative distributions of toluene, pyridine, and ethylbenzene increase over 201 days, while indole and methylindole decrease (Table 3). Despite the apparent loss of intracellular contents in the day 201 sample based on SEM, various protein-derived pyrolysis products were still observed albeit in lower abundance relative to the *n*-alkane/alk-1-ene products (Fig. 4D).

In the 4-Ma Pula kerogen, no detectable amount of proteinaceous substances was observed by conventional pyrolysis GC/MS. Using thermochemolysis with tetramethylammonium hydroxide, however, Mongenot et al. (2001), were able to detect amino acids and their derivatives in 140-Ma kerogen. We (Nguyen and Harvey,

1997, 2001) have also observed the presence of amino acids in Pula kerogen, by GC/MS of volatile derivatives of HCl hydrolyzates which will be reported elsewhere. These results indicate that any polar amino acid compounds found in highly degraded organic matter require a derivatization step prior to GC analysis.

3.4. ^{13}C NMR spectroscopy

The most intense signal in the NMR spectrum of the stationary-phase *B. braunii* culture (Fig. 5; day 0) is observed at a chemical shift of 30 ppm, representing aliphatic carbon. Other important signals are observed at 25 and 33 ppm (other paraffinic-C), 55 ppm (aliphatic C–N), 62 ppm (methoxyl-C), 72 ppm (alkoxy-C), 102 ppm (acetal- and ketal-C), 129 ppm (carbon and hydrogen substituted aromatic carbon; or isolated double bonds) and 174 ppm (carboxyl/amide-C). These signals correspond to the primary composition of algae, including proteins, carbohydrates, and lipids.

As observed in the pyrolysis gas chromatograms, enrichment in aliphatic material during the decay of *B. braunii* is observed in the ^{13}C NMR spectra. The paraffinic-C signals that persist in the NMR spectra throughout the 201-day degradation experiment are at 30 and 33 ppm (Fig. 5). The NMR spectra do not suggest any compositional changes in the paraffinic components from days 60 to 201, unlike the pyrolysis GC/MS technique, which indicates major compositional shifts (Table 3). These results support the notion that multiple approaches are needed in order to obtain a more comprehensive understanding of diagenetic changes.

The signals at 74, 102 and 173 ppm are still detected in the 201-day detritus albeit in significantly lower relative abundance compared to their contributions to the spectrum of stationary-phase algae. These spectral shifts indicate that biologically 'labile' substances, such as proteins and carbohydrates, are preferentially lost during diagenesis, with the preservation of aliphatic material likely from *B. braunii* cell walls. The peak at 130 ppm in the 201-day detritus may be assigned to an isolated unsaturated carbon in a long paraffinic chain such as those in algaenan, as this signal has been observed for chemically isolated algaenan (Blokker et al., 1998; Derenne et al., 1991; Gelin et al., 1996) and for the Pula kerogen (Fig. 5; and Derenne et al., 1997).

Because lipids, particularly fatty acids, are soluble in the organic solvents used to treat some of the samples, the missing 33-ppm signal in the spectra of the post-solvent extraction residues indicates the removal of these compounds (compare Figs. 5 and 6). The persistence of the 30-ppm peak in the post-solvent extraction residues indicates the retention of aliphatic-C corresponding to algaenans. These biomacromolecules, by definition, are not soluble in any organic solvent and would be expected to persist throughout the degradation sequence. The ^{13}C NMR spectrum of the solvent-treated day-201 residue (Fig. 6) appears more like that of isolated algaenan (Fig. 6). However, the presence of the carboxyl/amide-C signal at 172 ppm indicates that not all proteins are extractable with 0.1 N NaOH (at room temperature), as confirmed by 2D ^{15}N ^{13}C NMR (Zang et al., 2001).

4. Conclusions

The 201-day degradation study of *B. braunii* cell material using analytical pyrolysis and solid-state ^{13}C NMR clearly indicates that highly aliphatic material (i.e., algaenan) has been selectively preserved upon oxic decay. The resistance of this aliphatic material to microbial attack may largely explain the slower rate of organic matter decay for this green alga compared to other previously studied algae. Despite the apparent loss of intracellular contents for the 201-day detritus based on scanning electron microscopy, further molecular characterization revealed the retention of proteinaceous materials. The presence of such labile materials suggests that encapsulation (Knicker and Hatcher, 1997) or related mechanisms may be operative.

Acknowledgements

We thank Karl Dria (Ohio State Univ.) for assistance with NMR; Elaine Szymkowiak (Biology Department, St. Mary's College of Maryland) for assistance with SEM; Dr. Claude Largeau for the *Botryococcus* stock culture and valuable review comments on the manuscript; Paul del Giorgio (Horn Point Laboratory, UMCES) for performing the flow cytometry, and Dr. V. Grossi for reviewer comment. Financial support for this work was provided by the National Science Foundation (OCE-9896239 to PGH and OCE-9907069 to HRH), and the Ohio State University through a Graduate Student Award to X. Zang. Contribution 3627 of the University of Maryland Center for Environmental Sciences.

Associate Editor—**J. Sinninghe Damsté**

References

Allard, B., Casadevall, E., 1990. Carbohydrate composition and characterization of sugars from the green microalga *Botryococcus braunii*. Phytochemistry 29, 1875–1878.

Berkaloff, C., Casadevall, E., Largeau, C., Metzger, P., Peracca, S., Virlet, J., 1983. Hydrocarbon formation in the green alga *Botryococcus braunii*. Part 3. The resistant polymer of the walls of the hydrocarbon-rich alga *B. braunii*. Phytochemistry 22, 389–397.

Bertheas, O., Metzger, P., Largeau, C., 1999. A high molecular weight complex lipid, aliphatic polyaldehyde tetraterpenediol polyacetal from *Botryococcus braunii* (L race). Phytochemistry 50, 85–96.

Blokker, P., Schouten, S., van den Ende, H., de Leeuw, J.W., Hatcher, P.G., Sinninghe Damsté, J.S., 1998. Chemical structure of algaenans from the fresh water algae *Tetraedron minimum*, *Scenedesmus communis* and *Pediastrum boryanum*. Organic Geochemistry 29, 1453–1468.

Brock, T.D., Madigan, M.T., 1984. Biology of Microorganisms. Prentice Hall, Englewood Cliffs.

Cook, R.L., Langford, C.H., 1998. Structural characterization of a fulvic acid and a humic acid using solid-state ramp-CP-MAS ^{13}C nuclear magnetic resonance. Environmental Science and Technology 32, 719–725.

Dembitsky, V.M., Shkrob, I., Rozentsvet, O.A., 2000. Fatty acid amides from freshwater green alga *Rhizoclonium hieroglyphicum*. Phytochemistry 54, 965–967.

Derenne, S., Largeau, C., Casadevall, E., Sellier, N., 1990. Direct relationship between the resistant biopolymer and the tetraterpenic hydrocarbon in the lycopadiene-race of *Botryococcus braunii*. Phytochemistry 29, 2187–2192.

Derenne, S., Largeau, C., Casadevall, E., Berkaloff, C., Rousseau, B., 1991. Chemical evidence of kerogen formation in source rocks and oil shales via selective preservation of thin resistant outer walls of microalgae: origin of ultralaminae. Geochimica et Cosmochimica Acta 55, 1041–1050.

Derenne, S., Largeau, C., Hetényi, M., Brukner-Wein, A., Connan, J., Lugardon, B., 1997. Chemical structure of the organic matter in a Pliocene maar-type shale: implicated *Botryococcus* race strains and formation pathways. Geochimica et Cosmochimica Acta 61, 1879–1889.

Gelin, F., Boogers, I., Noordeloos, A.A.M., Sinninghe Damsté, J.S., Hatcher, P.G., de Leeuw, J.W., 1996. Novel, resistant microalgal polyethers: an important sink of organic carbon in the marine environment? Geochimica et Cosmochimica Acta 60, 1275–1280.

Gelin, F., Volkman, J.K., Largeau, C., Derenne, S., Sinninghe Damsté, J.S., de Leeuw, J.W., 1999. Distribution of aliphatic, nonhydrolyzable biopolymers in marine microalgae. Organic Geochemistry 30, 147–159.

Gillaizeau, B., Derenne, S., Largeau, C., Berkaloff, C., Rosseau, B., 1996. Source organisms and formation pathway of the kerogen of the Göynük oil shale (Oligocene, Turkey) as revealed by electron microscopy, spectroscopy and pyrolysis. Organic Geochemistry 24, 671–679.

Goth, K., de Leeuw, J.W., Püttmann, W., Tegelaar, E.W., 1988. Origin of Messel oil shale kerogen. Nature 336, 759–761.

Harvey, H.R., Macko, S.A., 1997. Kinetics of phytoplankton decay during simulated sedimentation: changes in lipids under oxic and anoxic conditions. Organic Geochemistry 27, 129–140.

Hatcher, P.G., Spiker, E.C., Szeverenyi, N.M., Maciel, G.E., 1983. Selective preservation and origin of petroleum-forming aquatic kerogen. Nature 305, 498–501.

Hedges, J.I., Stern, J.H., 1984. Carbon and nitrogen determinations of carbonate-containing solids. Limnology and Oceanography 29, 657–663.

Hetényi, M., 1976. Varsányi, contributions to the isolation of the kerogen in Hungarian oil shales. Acta Minerologica Petrographia 22, 231–239.

Kadouri, A., Derenne, S., Largeau, C., Casadevall, E., Berkaloff, C., 1988. Resistant biopolymer in the outer walls of *Botryococcus braunii*, B race. Phytochemistry 27, 551–557.

Kawasaki, W., Matsui, K., Akakabe, Y., Itai, N., Kajiwara, T., 1998. Volatiles from *Zostera marina*. Phytochemistry 47, 27–29.

Knicker, H., Hatcher, P.G., 1997. Survival of protein in an organic-rich sediment: possible protection by encapsulation in organic matter. Naturwissenschaften 84, 231–234.

Kröger, N., Bergsdorf, C., Sumper, M., 1994. A new calcium binding glycoprotein family constitutes a major diatom cell wall component. The EMBO Journal 13, 4676–4683.

Largeau, C., Casadevall, E., Kadouri, A., Metzger, P., 1984. Formation of *Botryococcus*-derived kerogens—comparative study of immature torbanites and of the extant alga *Botryococcus braunii*. Organic Geochemistry 6, 327–332.

Largeau, C., Derenne, S., Casadevall, E., Kadouri, A., Sellier, N., 1986. Pyrolysis of immature torbanite and of the resistant biopolymer (PRB A) isolated from extant alga *Botryococcus braunii*. Mechanism of formation and structure of torbanite. Organic Geochemistry 10, 1023–1032.

de Leeuw, J.W., Largeau, C., 1993. A review of macromolecular organic compounds that comprise living organisms and their role in kerogen, coal and petroleum formation. In: Engel, M.H., Macko, S.A. (Eds.), Organic Geochemistry. Plenum Press, New York, pp. 23–72.

Metzger, P., Casadevall, E., 1991. Botryococcoid ethers, ether lipids from *Botryococcus braunii*. Phytochemistry 30, 1439–1444.

Metzger, P., Largeau, C., 1999. Chemicals of *Botryococcus braunii*. In: Cohen, Z. (Ed.), Chemicals from Microalgae. Taylor and Francis, London, pp. 205–260.

Metzger, P., Villarreal-Rosales, E., Casadevall, E., Coute, A., 1989. Hydrocarbons, aldehydes and triacylglycerols in some strains of the A race of the green alga *Botryococcus braunii*. Phytochemistry 28, 2349–2353.

Mongenot, Th., Riboulleau, A., Garcette-Lepecq, A., Derenne, S., Pouet, Y., Baudin, F., Largeau, C., 2001. Occurrence of proteinaceous moieties in S- and O-rich Late Tithonian kerogen (Kashpir Oil Shales, Russia). Organic Geochemistry 32, 199–203.

Nguyen, R.T., Harvey, H.R., 1997. Protein and amino acid cycling during phytoplankton decomposition in oxic and anoxic waters. Organic Geochemistry 27, 115–128.

Nguyen, R.T., Harvey, H.R., 2001. Protein preservation in marine systems: hydrophobic and other non-covalent associations as major stabilizing forces. Geochimica et Cosmochimica Acta 65, 1467–1480.

Smucker, R.A., Dawson, R., 1986. Products of photosynthesis by marine phytoplankton: chitin in TCA "protein" precipitates. Journal of Experimental Marine Biology and Ecology 104, 143–152.

Stankiewicz, B.A., Hutchins, J.C., Thomson, R., Briggs, D.E.G., Evershed, R.P., 1997. Assessment of bog-body tissue preservation by pyrolysis-gas chromatography/mass spectrometry. Rapid Communications in Mass Spectrometry 11, 1884–1890.

Tegelaar, E.W., de Leeuw, J.W., Derenne, S., Largeau, C., 1989a. A reapparaisal of kerogen formation. Geochimica et Cosmochimica Acta 53, 3103–3106.

Tegelaar, E.W., Matthezing, R.M., Jansen, J.B.H., Horsfield,

B., de Leeuw, J.W., 1989b. Possible origin of *n*-alkanes in high-wax crude oils. Nature 342, 529–530.

Thompson, G.A., 1996. Lipids and membrane function in green algae. Biochimica et Biophysica Acta 1302, 17–45.

Tissot, B.P., Welte, D.H., 1978. Petroleum Formation and Occurrence. A New Approach to Oil and Gas Exploration. Springer-Verlag, Berlin.

Zang, X., Nguyen, R.T., Harvey, H.R., Knicker, H., Hatcher, P.G., 2001. Preservation of proteinaceous material during the degradation of the green alga *Botryococcus braunii*: a solid state 2D ^{15}N ^{13}C NMR spectroscopy study. Geochimica et Cosmochimica Acta 65, 3299–3305.

Zelibor Jr., J.L., Romankiw, L., Hatcher, P.G., Colwell, R.R., 1988. Comparative analysis of the chemical composition of mixed and pure cultures of green algae and their decomposed residues using ^{13}C nuclear magnetic resonance. Journal of Applied and Environmental Microbiology 54, 1051–1060.